Supporting Information

Tuning iron redox state inside a microporous porphyrinic metal organic framework

Brian Abeykoon[a], Jean-Marc Grenèche[b], Erwann Jeanneau[a], Dmitry Chernyshov[c], Christelle Goutaudier[a], Aude Demessence[d], Thomas Devic[e,f] and Alexandra Fateeva*[,a]

[a] *Université de Lyon, Université Claude Bernard Lyon 1, Laboratoire des Multimatériaux et Interfaces, UMR CNRS 5615, 43 Bd du 11 Novembre 1918, 69622 Villeurbanne, France*

[b] *Institut des Molécules et des Matériaux du Mans, UMR CNRS 6283 Université du Maine - Avenue Olivier Messiaen - 72085 Le Mans, France*

[c] *Swiss-Norwegian Beamline, ESRF BP-220, 38043 Grenoble, France*

[d]. *Institut de Recherches sur la Catalyse et l'Environnement de Lyon, Université Claude Bernard Lyon 1, UMR CNRS 5256, Villeurbanne, France*

[e] *Institut Lavoisier, UMR CNRS 8180, Université de Versailles Saint-Quentin-en-Yvelines, 45 avenue des Etats-Unis, 78035 Versailles cedex, France*

[f] *Institut des Matériaux de Nantes, 2 rue de la Houssinière, BP32229, 44322 Nantes cedex 3*

*To whom correspondence should be addressed: E-mail: alexandra.fateeva@univ-lyon1.fr

Contents:

Section 1: Chemicals and Instrumentations

All chemicals were obtained from commercial sources and used without further purification.

The linker TTPP (5,10,15,20-Tetrakis[4-(2,3,4,5-tetrazolyl)phenyl]porphyrin) was easily synthesized on a gram scale according to the reported procedure[1]

Note: (CAUTION! the synthesis procedure requires the use of sodium azide, handle with care to avoid explosive hazard)

Single crystal X-Ray diffraction on compound 1 was performed on the swiss-norvegian beamline at 250 K (λ = 0.95374 Å) using a PILATUS 2M detector. For compound 2 the data were obtained using a Gemini kappa-geometry diffractometer (Rigaku Oxford Diffraction) equipped with an Atlas CCD detector and using Mo radiation (λ= 0.71073 Å).

Powder X-Ray diffraction (PXRD) was performed on a PANanlytical XpertPro MRD diffractometer with a Cu Kα1 radiation (λ = 1.540598 Å) used with 40 kV and 30mA settings in θ/θ mode, reflection geometry. For the dried solids under inert atmosphere, Powder X-Ray diffraction (PXRD) was performed using a close sample holder on a Bruker D8 Advance diffractometer equipped with a Ge(111) monochromator producing Cu Kα1 radiation (λ = 1.540598 Å) and a LynxEye detector, in $\theta/2\theta$ mode, reflection geometry. High resolution PXRD pattern was collected at Cristal beamline at Soleil (λ = 0.79276 Å) using a sample suspended in DMF in a 0.7mm capillary, at 180 K. Le Bail refinement was performed using Jana2006 software.

The morphology of crystalline materials was observed by scanning electron microscopy on FEI Quanta 250 FEG and Zeiss Merlin Compact microscopes in the microscopy center of Lyon1 University. Samples were mounted on stainless pads and sputtered with ~2 nm of carbon to prevent charging during observation.

Thermogravimetric analysis (TGA) was performed with a TGA/DSC 1 STARe System from Mettler Toledo. Around 6 mg of sample is heated at a rate of 10 K·min-1 from 25 to 800 °C, in a 70 µl alumina crucible, under air atmosphere (20 mL.min^{-1}).

Infrared spectroscopy was performed with a Nicolet 380 FT-IR spectrometer coupled with the Attenuated Total Reflectance (ATR) accessory. Temperature dependent infrared analysis was carried out with a Nicolet iS10 FT-IR spectrometer equipped with a high temperature chamber. Data were collected from room temperature to 400°C with a data collection every 3 minutes and a heating rate of 2°C/min.

The supercritical CO_2 activation procedure was carried out using a Tousimis critical point dryer. The as-synthesized solid contained DMF in the pores hence liquid solvent exchange was performed with anhydrous ethanol during 4 cycles. In each cycle the solid was soaked in anhydrous ethanol for 24 hours, and then centrifuged and the solvent was replaced. The solid containing ethanol was then activated using a supercritical CO_2 dryer to prevent pores collapse due to capillary effect. About 40 mg of ethanol exchanged sample was loaded into a glass cell in the chamber. The chamber was then filled with liquid CO_2 and after 5 cycles of purge (5min) and soak steps, the temperature was elevated to obtain a supercritical CO_2 fluid. After 90 minutes, the bleed valve was slightly opened to allow a slow pressure decrease. When the pressure was low enough, the purge valve was opened and the chamber opened. The sample was finally loaded into a sorption cell.

Surface areas were measured by N_2 adsorption and desorption at 77.3 K using a BEL Japan Belsorp Mini apparatus volumetric adsorption analyzer. The sample was re-activated under secondary vacuum at 60°C prior to sorption measurement. The BET surface calculations was performed using points at the pressure range $0 < P/P^0 < 0.10$

The 57Fe Mössbauer spectra were recorded at 300 K and 77K in a transmission geometry using a 57Co/Rh source mounted on an electromagnetic drive with a triangular velocity form and a bath cryostat. The in-DMF sample was transferred into a sample holder usually used for ferrofluid measurements and immediately frozen under liquid nitrogen before introducing in the sample chamber of the cryostat to be thermalized at 77K, ready for measurements.

Section 2: Metal Organic Frameworks 1 and 2 synthesis procedure

Compound 1: $[Fe^{II}pzTTP(Fe^{II}_{1-x}DMF_{1-x}Fe^{III}_{x}OH_{x})]_n$

$FeCl_3.6H_2O$ (36 mg, 0.133 mmol), 5,10,15,20-Tetrakis[4-(2,3,4,5-tetrazolyl)phenyl]porphyrin (TTTP) (40 mg, 0.045 mmol) and pyrazine (10 mg, 0.13 mmol) were mixed in 5 mL of DMF and sealed in a pressure resistant vial. After stirring for 5 minutes at room temperature the reaction mixture was heated at 130°C for 48 hours (heating rate 0.3°C per minute, cooling rate: 0.3°C per minute). After cooling to room temperature purple crystals were recovered by centrifugation and washed with DMF until the solvent was colorless. After drying 30 mg of crystalline solid were recovered (yield ~ 55%). Due to stability issues the sample was stored either in DMF or dry under inert atmosphere.

Compound 2: $[Fe^{II}dabcoTTP(Fe^{II}_{1-x}DMF_{1-x}Fe^{III}_{x}OH_{x})]_n$

Compound 2 could be synthesized with the same procedure as compound 1 replacing the pyrazine with DABCO. However for the obtaining of single crystals the synthesis procedure was slightly modified as follows:

$FeCl_3.6H_2O$ (36 mg, 0.133 mmol), 5,10,15,20-Tetrakis[4-(2,3,4,5-tetrazolyl)phenyl]porphyrin (TTTP) (40 mg, 0.046 mmol) and pyrazine (15 mg, 0.13 mmol) were mixed in 5 mL of DMF and placed in a teflon reactor. After stirring for 5 minutes at room temperature the reaction mixture was sealed in a stainless steel reactor and heated at 160°C for 60 hours (heating rate 0.3°C per minute, cooling rate: 0.3°C per minute). After cooling to room temperature purple crystals were recovered by centrifugation and washed with DMF until the solvent was colorless. After drying 25 mg of crystalline solid were recovered (yield ~ 45%). Due to stability issues the sample was stored either in DMF or dry under inert atmosphere.

Section 3: Single crystal data refinement, distances, angles and bond valence sum tables

A single-crystal of compound 1 was mounted on a four-circle diffractometer of the BM01 beamline at the ESRF equipped with a Pilatus 2M detector and using a wavelength of 0.95374 Å.

A Suitable crystal of compound 2 was selected and mounted on a Gemini kappa-geometry diffractometer (Rigaku Oxford Diffraction) equipped with an Atlas CCD detector and using Mo radiation (λ= 0.71073 Å).

Intensities were collected at 250 K for compound 1 and 150 K for compound 2 by means of the CrysalisPro software[2].

Reflection indexing, unit-cell parameters refinement, Lorentz-polarization correction, peak integration and background determination were carried out with the CrysalisPro software[2]. An empirical absorption correction[2] was applied for compound 1 and an analytical one was applied to compound 2 using the modeled faces of the crystal[3]. The resulting set of *hkl* was used for structure solution and refinement.

The structures were solved by direct methods with SIR97[4] and the least-square refinement on F^2 was achieved with the CRYSTALS software[5].

The positions of all non-hydrogen atoms were refined anisotropically. The hydrogen atoms were all located in a difference map, but those attached to carbon atoms were repositioned geometrically.

The H atoms were initially refined with soft restraints on the bond lengths and angles to regularize their geometry (C---H in the range 0.93--0.98 Å) and U_{iso}(H) (in the range 1.2-1.5 times U_{eq} of the parent atom), after which the positions were refined with riding constraints.

Solvent accessible voids of 1445 $Å^3$ and 1531 $Å^3$ were found in the unit-cell of 1 and 2 respectively. The residual electronic density was present but could not be modelled thus its contribution was removed using the SQUEEZE algorithm[6].

Table S1: crystal data for compound 1 and 2:

	Compound 1	Compound 2
Chemical Formula	$C_{52}H_{24}Fe_3N_{22}O_2$	$C_{56}H_{48}Fe_3N_{22}O_2$
Z	2	2
M_r *(g.mol^{-1})*	1156.48	1228.68
Space Group	*Cmmm*	*Cmmm*
a (Å)	6.7530 (2)	7.160(2)
b (Å)	35.2750 (11) Å	34.398(11)
c (Å)	19.2653 (9) Å	19.626(4)
V (Å^3)	4589.2 (3)	4834(2)
T (K)	250	150
λ *(Å)*	*0.95374*	*0.71073*
Independent reflections /Parameters / Restraints	*1618 / 118 / 2*	*3339 / 133 / 20*
θ_{min} - θ_{max} (°)	2.1 - 31.8	2.9 – 29.4
$R[F^2 > 2\sigma(F^2)]$	0.053	0.089
$wR(F^2)$	0.135	0.276
GoF	0.96	1.01
$(\Delta/\sigma)_{max}$	0.0002	0.006
$\Delta\rangle_{max}$ (e.Å^{-3})	1.11	2.14
$\Delta\rangle_{min}$ (e.Å^{-3})	-0.53	-2.38

Table S2: selected distances (Å)

	Compound 1	Compound 2
Fe(2)-N(5)	2.147(3)	2.186(4)
Fe(2)-O(1)	2.018(3)	2.194(8)
Fe(2)-Fe(2)	3.3765(1)	3.580(1)
Fe(1)-N(3)	1.964(1)	2.267(1)
Fe(1)-N(1)	1.991(1)	2.009(1)
Fe(1)-N(2)	1.994(1)	2.015(1)

Table S3: selected angles (°)

	Compound 1	Compound 2
Fe(2)-O(1)-Fe(2)	113.581(1)	109.32(1)
N(5)Fe(2)-N(5)	86.11(18) 93.89(18)	87.4(1) 92.6(1)
N(5)-Fe(2)-O(1)	84.44(9) 95.56(9)	82.8(1) 97.1(1)

Table S4: bond valence sum calculation for Fe (2):

	Compound 1	Compound 2
Fe(2)-N(5)	2.147(3)	2.186(4)
Fe(2)-O(1)	2.018(3)	2.194(8)
BVS Fe^{II}	2.37	1.87
BVS Fe^{III}	2.62	2.09

	Carboxylate based compound [7]
Fe-O	2.012(1)
Fe-O	1.918(1)
BVS Fe^{II}	3.08
BVS Fe^{III}	3.29

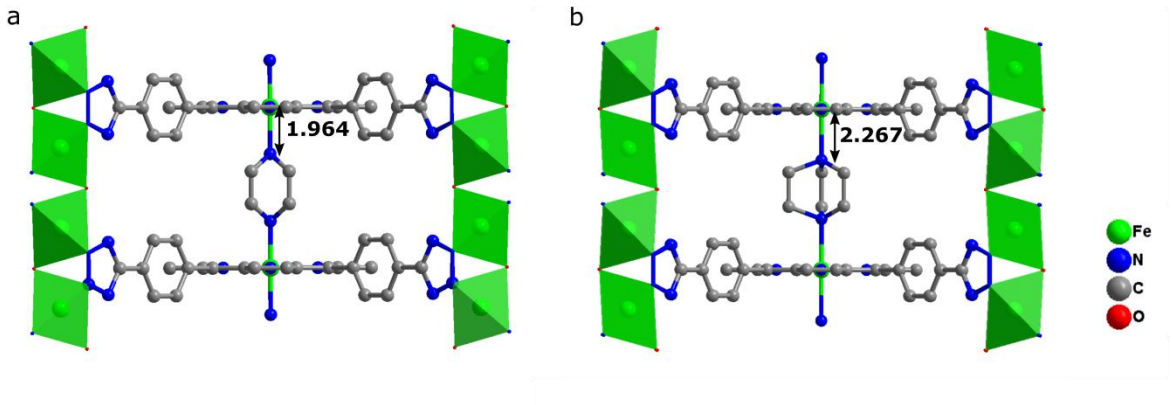

Figure S1 : bonds Fe-N bond length comparison in compound 1 and 2

Le Bail refinement:

Le Bail refinement was performed using Jana2006 software on the data recorded for sample suspended in DMF in a 0.7 mm capillary, at 180K. As initial model the cif file obtained from the structure solution from single crystal data collection (250K) was used.
The background was fitted with a 12 terms Chebyshev polynomial. The profile was fitted with a Pseud-Voigt peak-shape function. The zero-shift and the asymmetry (Simpson correction) were refined. The refined cell parameters are listed below:
a = 6.8420(3) Å, b = 35.883(3) Å, c = 19.069(2) Å
The refinement parameters are
GOF = 2.53, Rp = 6.14, wRp = 9.43.

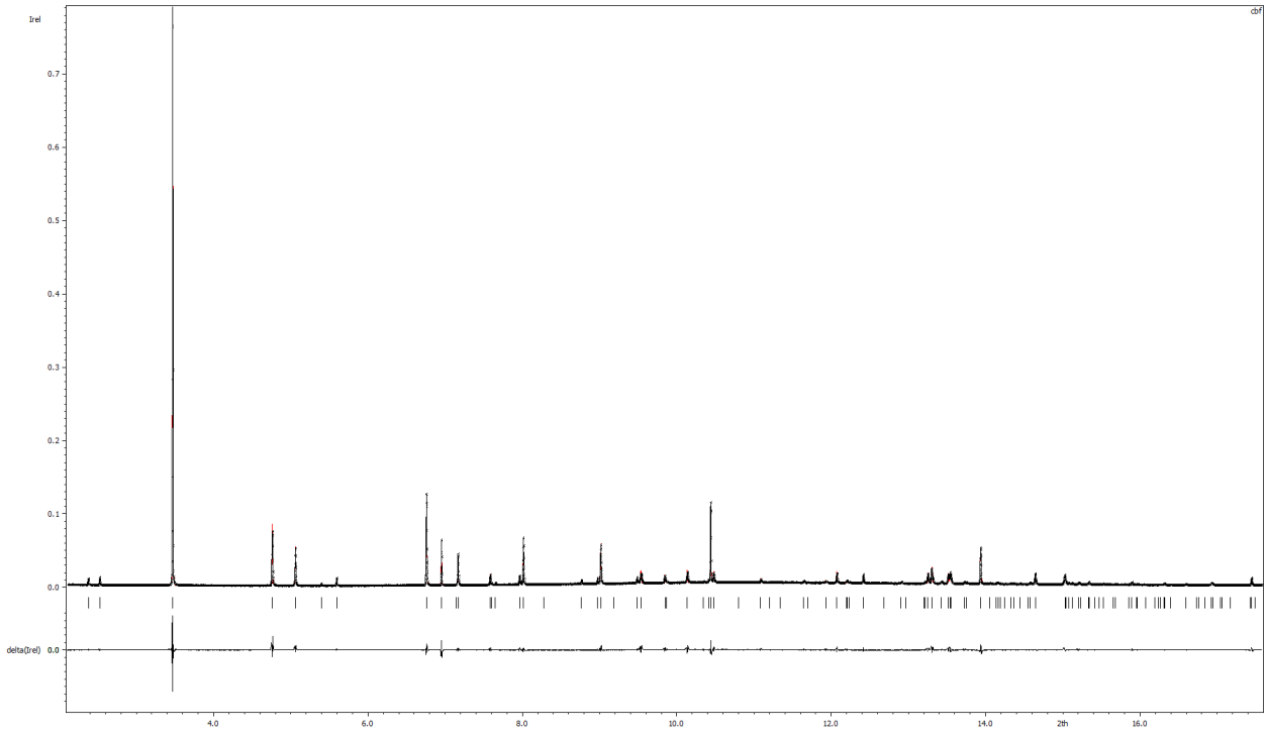

Figure S2 Le Bail pattern matching for compound 1

Section 4: FT-IR spectra

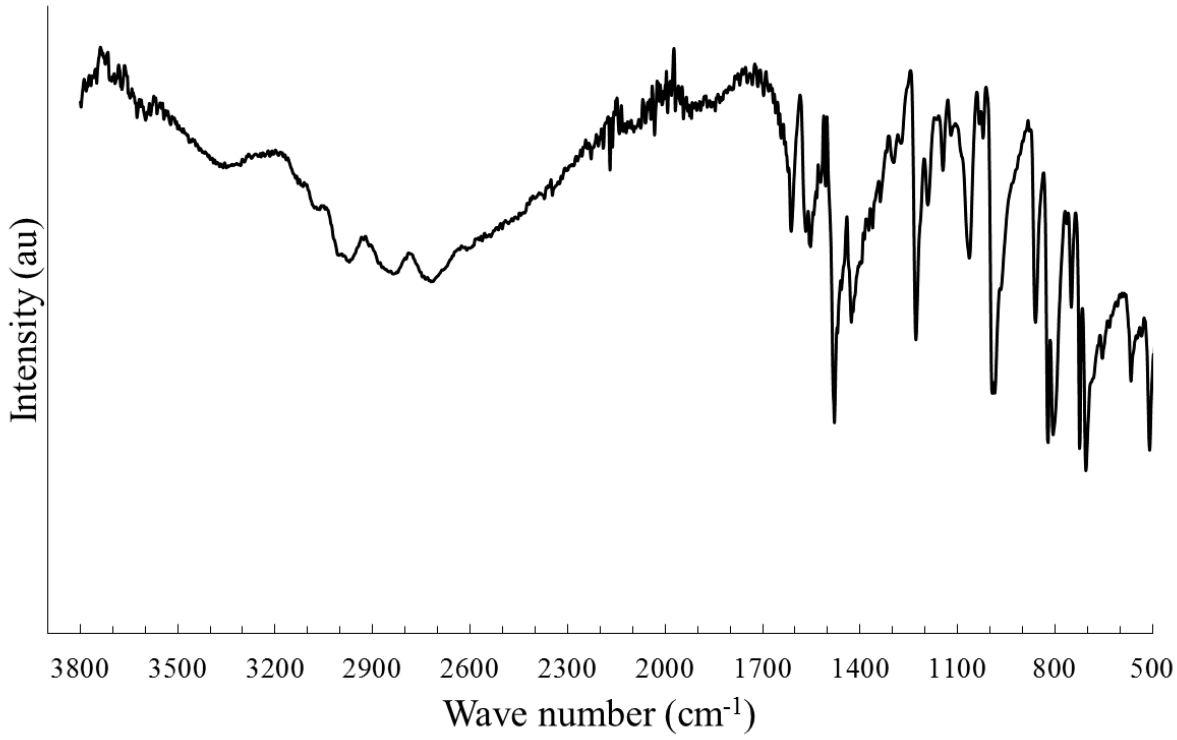

Figure S3 : IR spectrum of the H_2TTP ligand

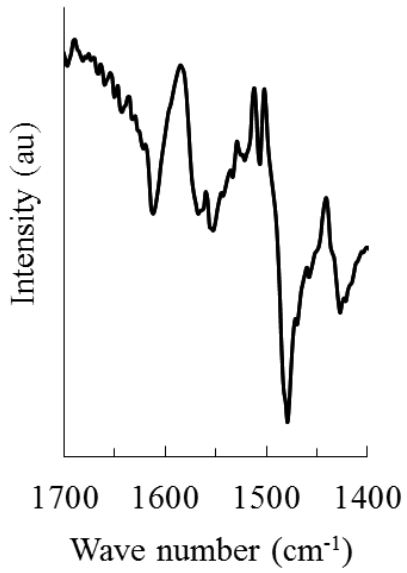

Figure S4. Inset on the IR spectrum of H_2TTPP showing the 1700-1400 cm^{-1} zone

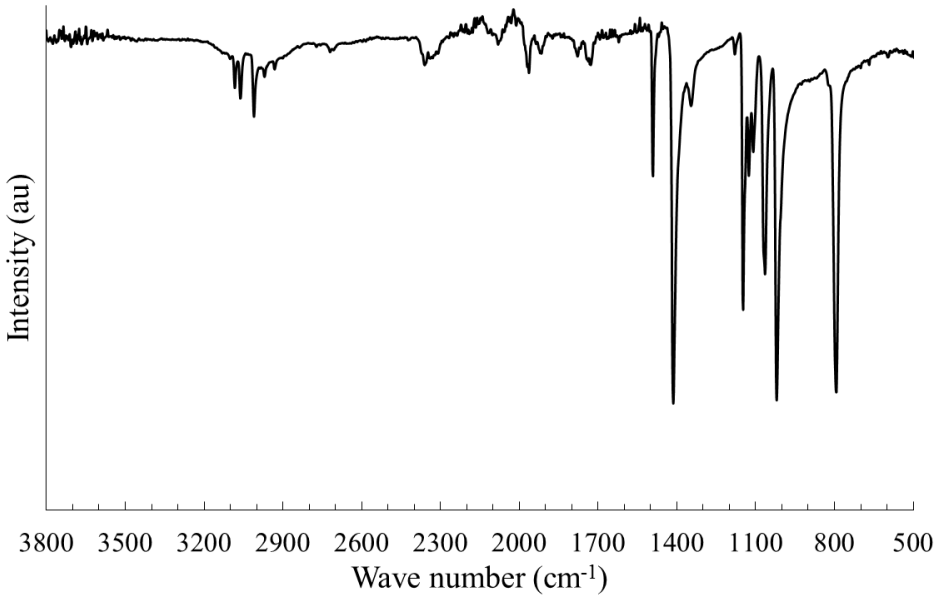

Figure S5 : IR spectrum of pyrazine

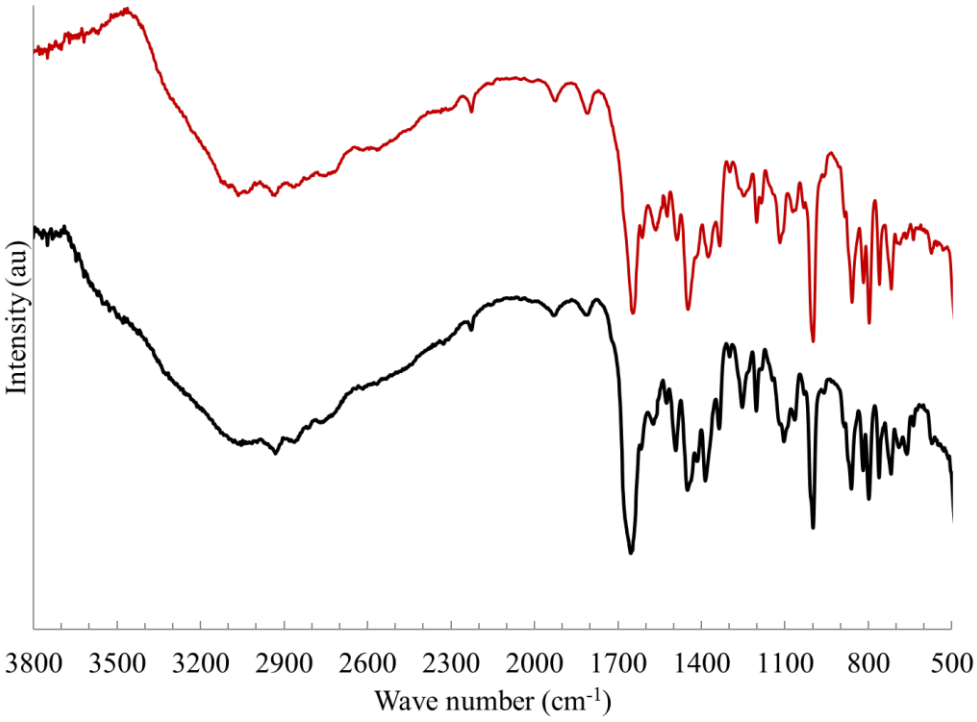

Figure S6 : IR spectrum of compound 1 as synthesised (black) and dried (red)

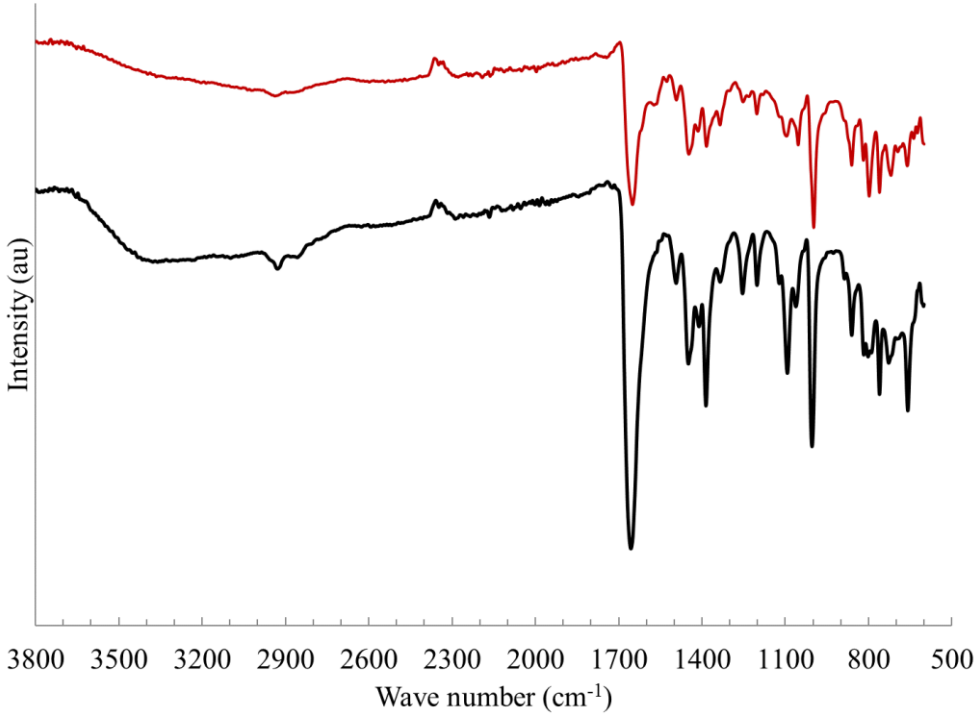

Figure S7 : IR spectrum of compound 2 as synthesised (black) and dried (red)

Section 5: Scanning Electron Microscopy

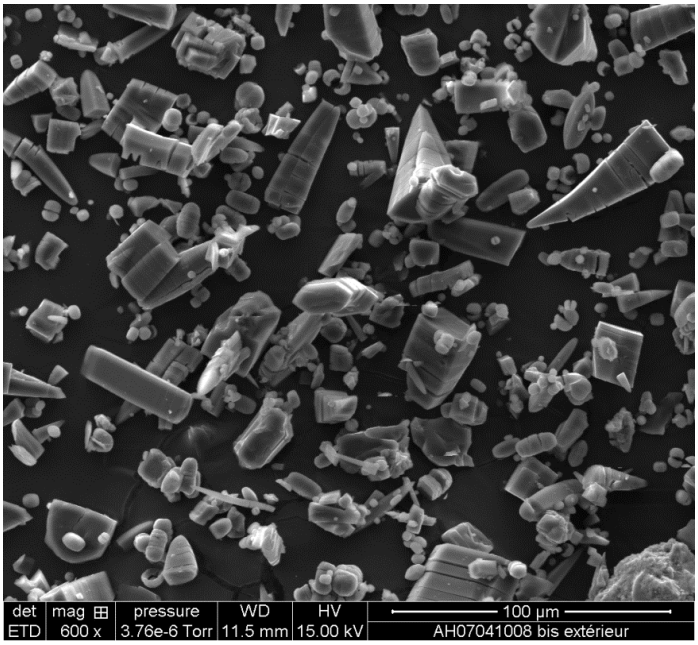

Figure S8. SEM image of compound 1

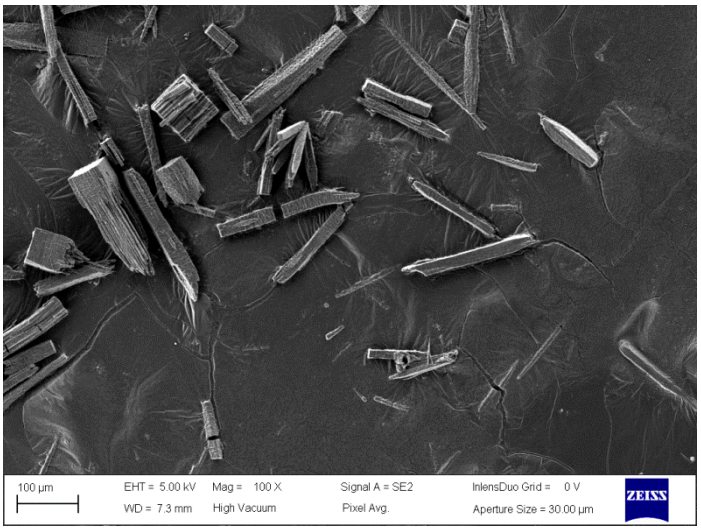

Figure S9 SEM image of compound 2

Section 6: Thermogravimetric analysis

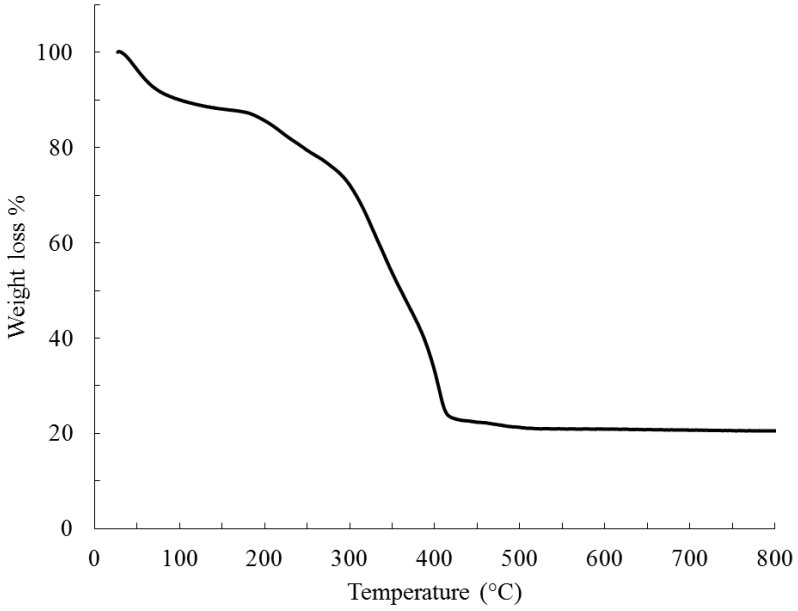

Figure S10. TGA data for compound 1

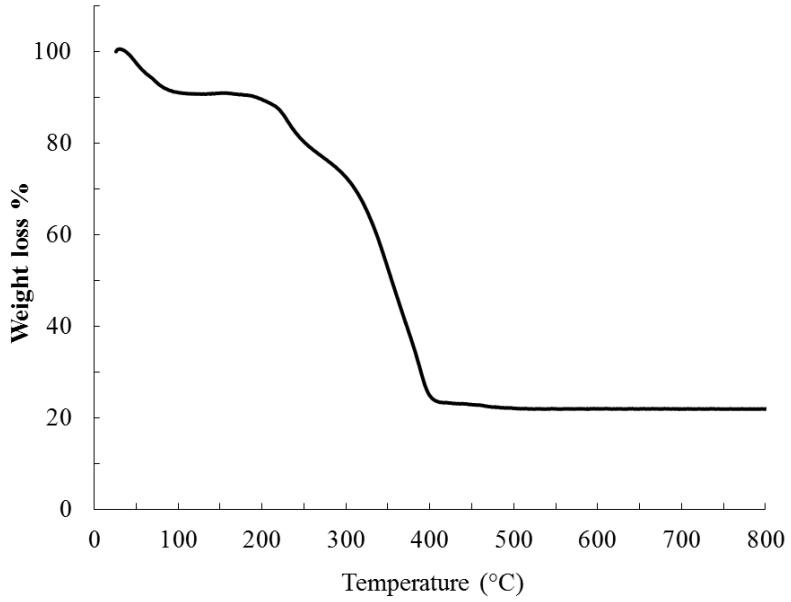

Figure S11. TGA data for compound 2

Section 7: PXRD data after nitrogen sorption isotherm measurement

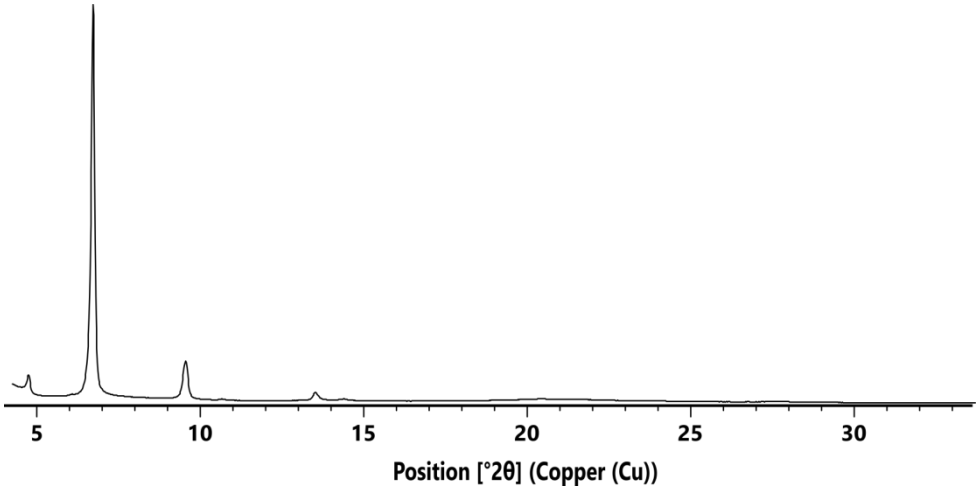

Figure S12. PXRD pattern of compound 1 after nitrogen sorption measurement

References

[1] P. J. F. Gauuan, M. P. Trova, L. Gregor-Boros, S. B. Bocckino, J. D. Crapo, B. J. Day, *Bioorganic & Medicinal Chemistry* **2002**, *10*, 3013-3021.

[2] *CrysAlisPRO, 1.171.38.43 Rigaku OD* **2015**.

[3] R. C. Clark, J. S. Reid, *Acta Crystallographica Section A* **1995**, *51*, 887-897.

[4] A. Altomare, M. C. Burla, M. Camalli, G. L. Cascarano, C. Giacovazzo, A. Guagliardi, A. G. G. Moliterni, G. Polidori, R. Spagna, *Journal of Applied Crystallography* **1999**, *32*, 115-119.

[5] P. W. Betteridge, J. R. Carruthers, R. I. Cooper, K. Prout, D. J. Watkin, *Journal of Applied Crystallography* **2003**, *36*, 1487.

[6] P. van der Sluis, A. L. Spek, *Acta Crystallographica Section A* **1990**, *46*, 194-201.

[7] A. Fateeva, J. Clarisse, G. Pilet, J.-M. Grenèche, F. Nouar, B. K. Abeykoon, F. Guegan, C. Goutaudier, D. Luneau, J. E. Warren, M. J. Rosseinsky, T. Devic, *Crystal Growth & Design* **2015**, *15*, 1819-1826.